3.4.2

ESS: The current beam design and target interface

M. Lindroos, M. Eshraqi
European Spallation Source, ESS, Lund, Sweden

Abstract. The ESS top level parameters of 5 MW, 3 ms pulse length and 14 Hz repetition rate are given by user requirements. The choice of 2 GeV, 62.5 mA and 2.87 ms pulse length were at laboratory level and were largely technology driven, e.g. the desire to keep beam current sufficiently low to avoid severe space charge issues resulting in the need of parallel front ends. After technology choices had been made, the final set of requirements resulting in the ESS 2013 lattice design were derived in an iterative process with cost and beam dynamics issues being the two main driving parameters. In large, cost was pushed to a minimum with emittance growth along the linac being used as a quality indicator. The beam is finally transported from the end of the last accelerating element to the target through a dogleg and is rastered over the target surface. We will in this paper review the ESS accelerator design process and will discuss the latest results mainly on the optics of the linac.

1. Introduction

The European Spallation Source, already under construction in Lund, Sweden, has been financed to be a facility with the single purpose of providing spallation neutrons to users and therefore the design parameters have been heavily affected by the requirements dictated by neutron users. These parameters, the high level requirements, are the unprecedented power of 5 MW, a beam pulse of $\sim$ 3 ms and a repetition rate of 14 Hz. The choice of final beam energy of 2.0 GeV and 62.5 mA of beam current are however technology and cost driven. For example a higher beam energy increases the cost of the linac [1] and increasing the beam current strengthens the space-charge non-linear forces that could lead to increased halo growth and higher chance of beam loss. The selection of a reasonable beam energy and current which keeps the linac costs limited while the risk of beam losses is still manageable is discussed in detail in [1].

The ESS linac accelerates 62.5 mA of protons up to 2 GeV in a sequence of normal conducting and superconducting accelerating structures and eventually paints a tungsten target with this beam where a high flux of neutrons will be generated in a neutron rich target material at the same pulse rate as the proton beam. The proton pulses are 2.86 ms long with a repetition rate of 14 Hz − corresponding to a duty cycle of 4%. These parameters are high level parameters which affect the design and geometry of the instruments and the neutron guides.

Hands-on maintenance and machine protection set limits of 1 W/m and 0.1 W/dm respectively, on beam losses and have been a concern in every high power linac. In the ESS case a loss at such a level is in the order of 10^{-7} with respect to the total beam power. Therefore it is very important to design the accelerator, specially for high power accelerators, such that it does not excite particles to beam halo.

At a frequency of 352.21 MHz a 62.5 mA beam has $\sim$ 1.1×10^9 protons per bunch. From $\sim$ 200 MeV onward the acceleration is done at twice the frequency of the front end, 704.42 MHz,

to improve the energy efficiency of the linac. The frequencies, transition energies and structures are schematically shown in figure 1.

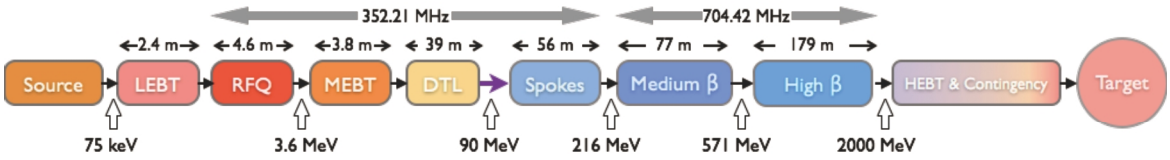

Figure 1: Block layout of the ESS baseline linac 2013, OptimusPlus (not to scale). Warm colored boxes represent the normal conducting components and cold color boxes the superconducting sections.

2. Architecture

2.1. Ion Source and LEBT

The high intensity beam of protons is produced by a Microwave Discharge Ion Source, MDIS. The beam pulse generated by the proton source is up to 3 ms long with an energy of 75 keV and a proton intensity exceeding 80 mA at the source exit. These type of ion sources have a high reliability just shy of 100% and a long mean time between failures, MTBF. The high reliability of these sources has already been demonstrated in similar ion sources [2]. The source is followed by the Low Energy Beam Transport, LEBT, which is composed of two magnetic solenoids that match the beam to the downstream RFQ, a chopper system that removes low quality head and tail of the beam, an iris that is used to generate different (lower) beam currents, and a set of beam diagnostics that measures the beam before it is injected to the linac.

2.2. RFQ

The four-vane RFQ as the first rf accelerating structure in the ESS linac, accelerates, focuses, and bunches the continuous 75 keV beam to 3.62 MeV within 4.6 m [3]. The output energy of the RFQ has increased in this layout from 3 MeV to 3.62 MeV in a process of optimizing all the transition energies in the linac. The beam current at the exit of the RFQ under nominal operation modes should be 62.5 mA, which taking into account the nominal transmission of 98%, the input beam should be at least 64 mA. The rf frequency of the RFQ and hence the bunches is 352.21 MHz. The peak electric fields on the vane surface has been limited to a Kilpatrick value of 1.6.

2.3. MEBT

A medium energy beam transport between the RFQ and the DTL transports and matches the beam out of the former structure to the latter one, provides means to collimate the beam, measures the beam's transverse and longitudinal profile and chops off the remaining low quality bunches which couldn't have been cleaned out by the LEBT chopper. The MEBT is composed of 11 quadrupoles, three buncher cavities, a chopper with its correspondent dump system, 3 sets of 4 independent collimating plates and beam diagnostics.

2.4. DTL

The drift tube linac brings the beam energy to 89.6 MeV in five tanks [4]. Each tank is fed by a 2.8 MW klystron, having left a 30% margin for LLRF, tuning and waveguide losses, 2.2 MW

of power is delivered to the cavity via two rf windows, almost 50% of which is transferred to the beam. Higher input energy to the DTL resulted in longer input cells with several positive consequences; longer cells could house bigger quadrupoles reducing their magnetic gradient for the same integrated gradient, have longer gaps reducing the field at the flat of the drift tube due to magnets and also rf, and enhances the effective shunt impedance, ZTT. The transverse focusing is still provided by permanent magnet quadrupoles, PMQs, that are housed in every other drift tube. Three corrector dipoles per plane per tank are correcting the beam center. The constraints present in a DTL required an optimization process on where to put these corrector dipoles.

2.5. Spoke Section

The DTL is the last normal conducting structure, and right after it comes the Low Energy Differential Pumping section, LEDP, that is used to create the required vacuum quality at the transition to superconducting cavities. The spoke cavities are used to accelerate the beam from 89.6 MeV to 216 MeV. One of the reasons for choosing spoke cavities instead of the conventional normalconducting structures in this energy range is their relatively large transverse aperture and tune-ability for different phase and energy beams. These 352.21 MHz double-spoke cavities with an optimum β of 0.50 are housed in pairs in 13 cryomodules, and are separated by spoke warm units, SWU. Every SWU is composed of a pair of quadrupoles each being equipped with a single plane corrector and a beam position monitor, and a central slot allocated to beam diagnostics [5].

2.6. Elliptical Sections

The rf frequency doubles to 704.42 MHz at the beginning of the next structure, the medium-β elliptical cavities. There are two families of elliptical cavities accelerating the beam from the spoke output energy to 571 MeV using 36 medium-β cavities and further to 2.0 GeV by 84 high-β cavities. In both sections four cavities are housed in cryomodules of identical length. Having different geometric βs of 0.67 and 0.86 respectively, the medium-β cavities are given an extra cell (6-cell) with respect to high-β cavities (5-cell) to have almost the same length. This has been done to achieve the same period length in the medium and high-β sections, making them swap-able in case the required gradient in medium-β is not achieved. There are identical elliptical warm units, EWUs, before each cryomodule. These EWUs have the same functionality as SWUs, with bigger apertures, and longer quadrupoles. To have the same flexibility at the spoke to medium-β transition the period lengths in elliptical section is chosen to be exactly twice that of the spoke section [5].

2.7. HEBT

The same periodicity, in transverse plane, is maintained for 15 periods after the high-β section in the high energy beam transport, HEBT, for contingency purposes. After this contingency area, there is one more EWU which is followed by a vertical dipole with a bending angle of 4° that also works as a switch magnet between the beam dump and the target. The beam going to the target is bent downward to horizontal plane using a second vertical dipole after 6 periods of longer doublet focused sections that are adjusted to create an achromat dogleg. This beam is transported to the target using a set of quadrupoles and 8 raster magnets that paint the target surface in horizontal and vertical directions at different frequencies [6]. To reduce the beam center movement on target due to energy jitter the phase advance between the second dipole and the target surface is set to be a multiple of 180°. A fixed collimator may intercept beam halo, protecting edges of the target, and also stops the back scattered neutrons from target. When the beam is directed to the 12.5 kW beam dump (The first dipole switch off) the beam is magnified on to the dump entrance face using three quadrupoles.

2.7.1. Raster system The beam density on the surface of the target is desired to be as uniform as possible to achieve the lowest peak density. One can either use a non-linear magnetic system to achieve this goal (very distribution dependent) or paint the area with the beam. The ESS HEBT uses a fast horizontal-vertical sweeping system, dubbed raster system, to achieve this goal. The raster system is composed of four dithering dipole magnets per plane which sweeps the beam on the target surface within the 2.86 ms pulse, shaping a rectangle of 180×60 mm^2 (H×V) with almost a uniform density within the footprint that drops to zero at the same rate as the initial beam out of linac does [7]. These magnets are driven by two triangular waveform currents with frequencies of up to 40 kHz.

3. Beam dynamics

3.1. Design Criteria

In the latest design one of the main goals was to keep the cost of the accelerator at the budget, a linac that had a lower final energy, but higher current to keep the power constant. Increased beam current would have increased the effect of space-charge and therefore a study was performed to lower the effect of space-charge without increasing the cost [8]. Following this paper [8], the relative tune spread ($\zeta = 1 - \sigma/\sigma_0$), where σ and σ_0 are the phase advances with and without current respectively, is kept below 0.6 (limiting the number of mismatch resonances to only two) while the current is increased by 25%, see Fig. 2.

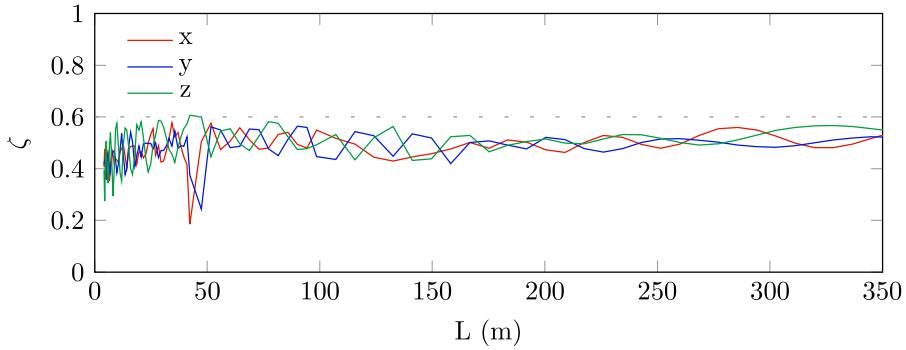

Figure 2: Relative tune spread along the linac, the dotted line marks the 0.6 limit.

The ESS linac will accelerate beam currents from 6.5 mA to 62.5 mA, therefore a smooth and monotonic variation of the phase advance per meter not only improves the matching, it also shortens the tuning time for different beam currents. On top of this, the structures are matched by smoothing the phase-advance variation at transitions to assure a good beam quality throughout the accelerator, even with different beam currents. The transverse phase advance per period is limited to 87° to reduce the percentage of the beam that due to their phase otherwise would have had a phase advance exceeding 90° per period.
To improve the acceleration efficiency, the longitudinal phase advance per period is limited throughout the linac to85°, a limit which is reached only in the medium β section. On top of the transverse aperture, the longitudinal acceptance has also been kept large not to cause longitudinal losses which eventually result in transverse losses.

Tracking a beam of 100,000 macro-particles with a gaussian distribution in 4D and truncated at $4 \times \sigma$ from the RFQ input to the target shows the beam behavior under perfect settings. This tracking is performed using the code TraceWin [9]. The envelopes stay confined well within the aperture and no significant emittance growth is observed in the linac, see figure 3. The halo values stay also confined with this design, removing the need for a collimation system.

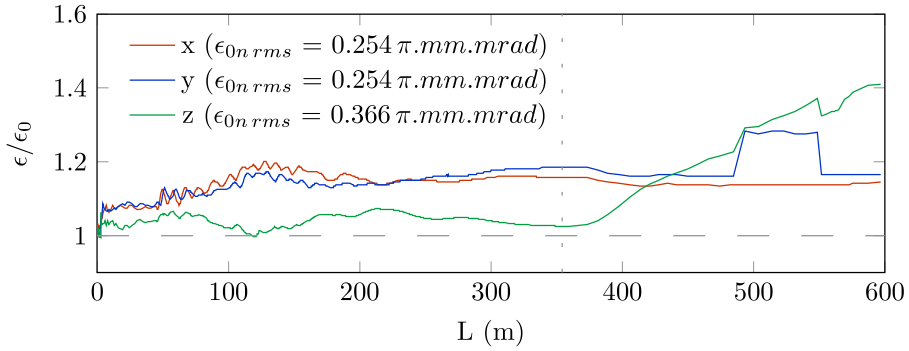

Figure 3: RMS emittance growth with respect to input beam along the linac and HEBT. Vertical dotted line shows the end of linac/start of HEBT.

4. Summary

The ESS linac is designed through a collaboration with several institutes and universities. Even with a reasonably high beam current an integrated and careful design of the linac beam dynamics assures that the beam quality along the linac is not degraded and losses are avoided. The high quality beam is swept on the neutron production target surface to create a uniform beam using a set of high frequency dipole magnets.

[1] D. McGinnis, "New Design Approaches for High Intensity Superconducting Linacs - the New ESS Linac Design", *in proceedings of* IPAC 2014, Dresden, Germany.
[2] L. Celona et al., Rev. Sci. Instrum. 75, 5 (2004).
[3] A. Ponton, "Note on the ESS RFQ Design Update", ESS Technical Report, 2014.
[4] R. D. Prisco, *et.al.*, "ESS DTL Status: Redesign and optimizations", *in proceedings of* IPAC 2014, Dresden, Germany.
[5] M. Eshraqi, "Beam physics design of the Optimus+ SC linac", eval.esss.lu.se/DocDB/0003/000309/003/OptimusPlus.pdf.
[6] H. D. Thomsen, S. P. Møller, "The ESS High Energy Beam Transport after the 2013 Design Update", *in proceedings of* IPAC 2014, Dresden, Germany.
[7] H. D. Thomsen, S. P. Møller, "The Design of the Fast Raster System for the European Spallation Source", *in proceedings of* IPAC 2014, Dresden, Germany.
[8] M. Eshraqi, J,-M, Lagniel, "On the choice of linac parameters for minimal beam losses", IPAC2013.
[9] R. Duperrier, N. Pichoff and D. Uriot, Proc. International Conf. on Computational Science, Amsterdam, The Netherlands, 2002.